Atmospheric and Climate Sciences, 2025, 15(1), 275-288
https://www.scirp.org/journal/acs
ISSN Online: 2160-0422
ISSN Print: 2160-0414

A Year-Round Study of Water Vapor, Energy and Net Ecosystem Exchanges in a Young Oil Palm Field in Dangbo, Bénin

Ossénatou Mamadou

Institut de Mathématiques et de Sciences Physiques, Dangbo, Bénin
Email: ossenatou.mamadou@imsp-uac.org

How to cite this paper: Mamadou, O. (2025) A Year-Round Study of Water Vapor, Energy and Net Ecosystem Exchanges in a Young Oil Palm Field in Dangbo, Bénin. *Atmospheric and Climate Sciences*, **15**, 275-288.
https://doi.org/10.4236/acs.2025.151013

Received: August 25, 2024
Accepted: January 28, 2025
Published: January 31, 2025

Copyright © 2025 by author(s) and Scientific Research Publishing Inc.
This work is licensed under the Creative Commons Attribution International License (CC BY 4.0).
http://creativecommons.org/licenses/by/4.0/
Open Access

Abstract

In 2022, an eddy covariance site was established in a young oil palm plantation in southeast Dangbo, Bénin, to study the exchange of CO_2, energy, and water vapor. This study aims to present the first one-year analysis of seasonal dynamics in energy balance components and net ecosystem exchange above this type of ecosystem in Africa. The first results show that on average during the 2023 year, 55% of net radiation is consumed into actual evapotranspiration, demonstrating the significant amount of latent heat flux in the energy balance, as expected at this tropical humid site. The sensible heat flux was substantial, ranging between 60 and 200 $W \cdot m^{-2}$, while net radiation varied between 440 and 650 $W \cdot m^{-2}$. Carbon uptake and net release of CO_2 into the atmosphere were permanent at the site. However, the CO_2 uptake increases more when rainy events become regular. On average, the mean nighttime CO_2 flux was ~8 $\mu mol \cdot m^{-2} \cdot s^{-1}$, while during the daytime it was ~−20 $\mu mol \cdot m^{-2} \cdot s^{-1}$.

Keywords

Net Ecosystem Exchange, Water Vapor Loss, Available Energy, Palm Oil, Benin, West Africa

1. Introduction

In Benin, oil palm plays an important economic role and is the most productive oil crop. Due to its importance in the economy and food security of rural communities, there is nowadays a huge expansion of village palm plantations. Knowing that the environmental impacts of such a plantation are currently a highly controversial topic [1]-[3], this study responds to the need to understand the dynamic of carbon dioxide exchange from this ecosystem into the atmosphere in southeastern Benin. While the Intergovernmental Panel on Climate Change demonstrates the link between greenhouse gas emissions from anthropogenic sources and global warming [4]-[6], each economic actor seeks virtuous arguments by announcing their relative carbon neutrality [7]-[10], often by offsetting their carbon dioxide (CO_2) emissions through the planting of hectares of forest [11]. Despite the fact that these actions can be considered as an illusion and do not encourage changes, carbon sequestration of some ecosystems is still uncertain, especially in tropical humid areas, particularly in Africa, where few stations are deployed [12].

Regarding cultures having the most economic relevance, palm oil, an oleaginous crop, provides 39% of vegetable oil world production with 7% of oleaginous plantation areas compared with soybean (61%), colza (18%), and sunflower (14%) [13]. In Benin, palm oil occupies a predominant position in agricultural production, trade, and consumption of fats [14]. Due to its importance in the economy and food security of rural communities, the Beninese government, through its development project, launched in 2020 an official program that supports palm oil plantations within the country. Whilst the global demand is projected to double by 2030 [15], it is also expected that palm oil plantations will tend to expand in order to meet this demand. However, the land cover changes that this expansion will induce will probably lead to changes in the earth system through among others albedo, surface temperature, carbon dioxide, sensible heat and evapotranspiration exchanges [16]-[20].

Many studies have focused on surface ecosystem exchanges using the eddy covariance technique worldwide [21]-[23]. However, in the West African tropical humid region, water vapor, CO_2 and energy fluxes were first analyzed by [19] [20] [24]-[26]. In northern Benin, the first study was conducted by [20], who investigated water vapor and energy fluxes over one year (2008) above a cultivated area and later compared the dynamics of two contrasting vegetation types over two years [19]. The authors pointed out 1) contrasted surface responses depending on the season and 2) the importance of surface temperature, which directly drives the longwave radiation budget and indirectly the water vapor fluxes through transpiration limitations. The CO_2 flux response to climatic and edaphic factors was studied over a cultivated area, a degraded woodland, and above a clear forest by [25] [27] [28]. Soil moisture was the main controlling factor of ecosystem CO_2 dynamics with a larger uptake in the wet compared to the dry season [25] [27] [28]. The CO_2 fluxes over the clear forest were always higher than those of cultivated savannah [28] and the degraded woodland was close to an equilibrium state according to its carbon exchanges with the atmosphere [27].

To our knowledge, no study has reported on the ecosystem scale CO_2 and H_2O of palm oil plantations in Africa using eddy covariance measurements. The objective of this study is to highlight one year (2023) dynamics of energy, water vapor and net ecosystem exchanges from this ecosystem located in a sub-equatorial climate (southeast Benin) also called the "tropical savanna climate (Aw) according to the classification Köppen-Geiger" [29], ~54 km away from the Atlantic Ocean (Figure 1). The materials and method used are presented in Section 2, and the preliminary results are examined and discussed in Section 3. The last section concludes this study.

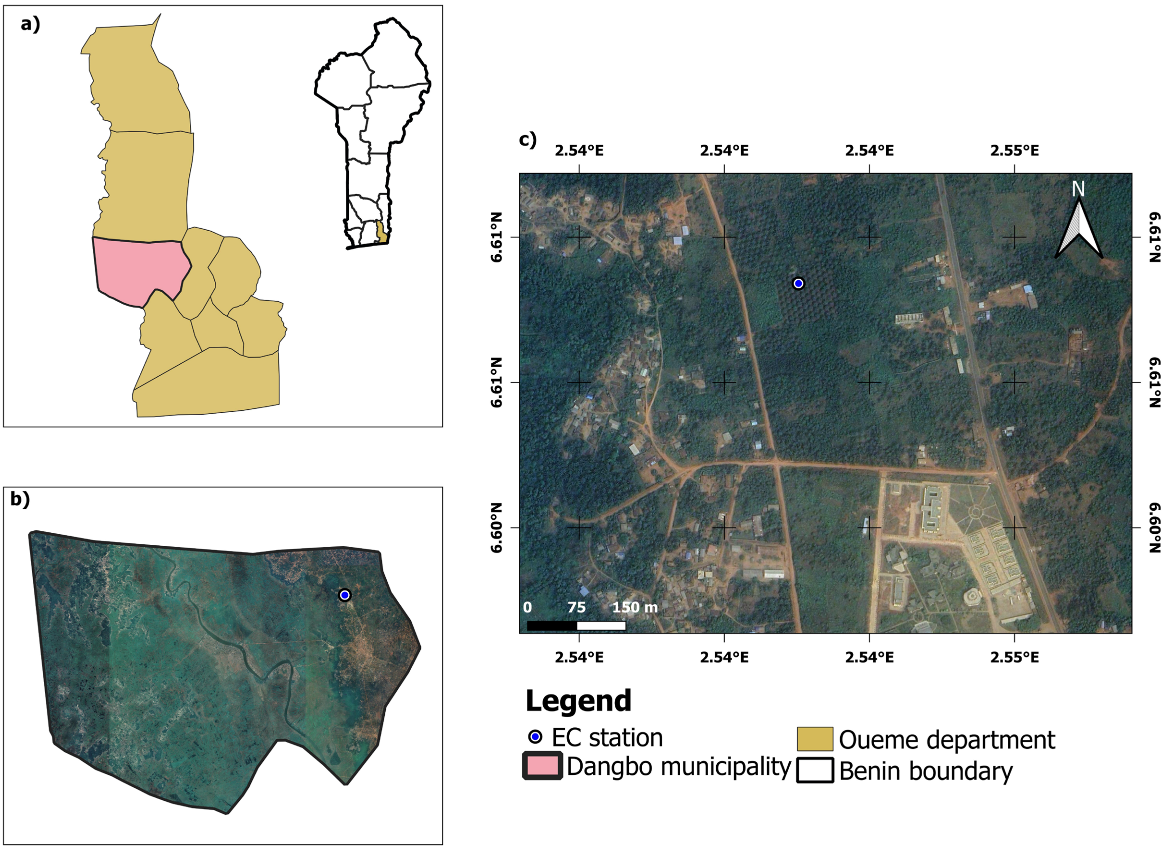

Figure 1. Geographical location of: (a) the Ouémé department and Dangbo municipality in Benin; (b) the eddy covariance site in the Dangbo municipality; (c) the Google earth view of the study site, the blue circle indicated the location of the flux tower.

2. Materials and Method

2.1. Description of the Site and Instrumentation

The study site is a young (~5 years old) palm oil plantation in Dangbo (latitude 6.607˚N, longitude 2.543˚E), a tropical humid region within the Ouémé Valley, the second most fertile valley in the world after the Nile. The eddy covariance site is located less than 2 km away near the "Institut de Mathématiques et de Sciences Physiques" and has been funded by the UNESCO OWSD Early Career Fellowship under the ASEEW@ (Assessment of Surface Ecosystems Exchanges in West Africa) research project. The climate of the region is sub-equatorial Guinean, characterized by consistently high temperature (air and soil) and high relative humidity (>50%) throughout the year [30]. This climate type is also called, according to the Köppen-Geiger classification, a tropical savanna climate (Aw) [29]. The Dangbo's region is characterized by the alternation of two wet (rainy) seasons alternating with a long dry season (December-February) and a short dry season (July-August), which rarely exceeds two months [30]. The relief of the region has two geomorphological units: a plateau at altitudes of between 20 and 200 m, with pronounced undulations, and a floodplain no more than 10 m above sea level, in the north-south direction and adjoining the plateau in the east-west "toposequence" [31]. The dominant soils on the plateau where the flux tower is located are "ferrallitic soils" [32].

2.2. Measurement of CO_2, H_2O and Energy Fluxes and Environmental Variables

Fluxes of energy, CO_2 and H_2O were measured by the eddy covariance technique using a 3D sonic anemometer (CSAT3B, Campbell Scientific Inc.), and an open-path CO_2/H_2O analyser (LI-7500A, Li-Cor Inc.), installed toward the predominant winds from southeast at a height of 9.2 m. The signals of the sensors were sampled at a frequency of 20 Hz. Measurements of this system comprise the wind speed in the three directions (u, v, w), the sonic temperature, water vapor and CO_2 molar densities. In addition, downward and upward shortwave and longwave radiation components were measured using a radiometer (CNR4, Kipp & Zonen). One heat flux plate (HFP01SC, Hukseflux Thermal Sensors, Delft, The Netherlands) was buried 0.01 below the surface to measure soil heat flux. The HygroVue 5 (Campbell Scientific) was employed to measure air temperature and relative humidity whereas the WindSonic4 (Campbell Scientific), a 2-D Sonic Wind Sensor, is used to measuring wind speed and wind direction. Soil electrical conductivity, relative dielectric permittivity, volumetric water content and soil temperature in the top 5 cm, 10 cm, 20 cm and 30 cm thick layers respectively, were measured using TDR sensors (CS650, Campbell). Precipitation was measured at 1 m above the ground using an unheated tipping-bucket rain gauge. All the environmental variables were measured every 10 s and recorded every 5 min.

2.3. Data Processing and Flux Computation

All flux data are processed with the EddyPro (v7.0.6) software with the following settings: 1) flux averaging is set to 30 min and raw data containing 30% of gaps are not used to compute fluxes; 2) double rotation to align the sonic anemometer with the streamlines; 3) density correction for sonic temperature after [33]; 4) high frequency spectral corrections after [34] and 5) quality control tests based on approach developed by [35]. After EddyPro, all abnormal data generally caused by instrument malfunction and sonic anemometer error generated often by rainy events, were excluded during flux data processing. In this study, data measured from 1 January 2023 to 31 December 2023 were used for analysis.

The sensible heat (H) and water vapor (LE) fluxes are calculated (Equations (1) and (2)) as the covariance between the fluctuation of the wind speed in the vertical direction w'(m·s^{-1}) and the fluctuation of the temperature T'(K) for the sensible heat and the fluctuation of the absolute air humidity q'(g·m^{-3}) for the latent heat.

In Equations (1) and (2), ρ (kg·m^{-3}) is the density of dry air at a given air temperature; Cp (J·kg^{-1}·K^{-1}), the specific heat at constant pressure and λ [J·g^{-1}], the latent heat of vaporization of water.

$$H = \rho C_p \overline{w'T'} \tag{1}$$

$$LE = \lambda \overline{w'q'}. \tag{2}$$

The station also includes measurements of the four components of the radiation balance allowing thus the estimation of the energy balance (Equation (3)), an independent diagnosis to check the consistency of H and LE computed from (Equations (1), (2)).

$$Rnet - G = H + LE \tag{3}$$

$Rnet$ is the net radiation (W·m^{-2}) and G the ground heat flux (W·m^{-2}) measured by the heat flux plate. The net radiation was calculated from measured incoming and outgoing short- and longwave radiations.

From some simplification of the conservation of mass balance equation [36], net ecosystem exchange (NEE, µmol·m^{-2}·s^{-1}) was calculated as the sum of the turbulent vertical flux (F_C, µmol·m^{-2}·s^{-1}) measured by the eddy covariance system at the reference height z (m) and the rate of change in storage of CO_2 (S_C, µmol·m^{-2}·s^{-1}), estimated from CO_2 measurements at the reference height (Equation (4))

$$NEE = F_C + S_C = \frac{1}{V}\overline{w'c'} + \int_0^z \frac{1}{V}\frac{\partial \overline{c}}{\partial t}\mathrm{d}z \tag{4}$$

V is the molar volume of the dry air (m^3·mol^{-1}), c the molar fraction (µmol·mol^{-1}), t the time (s). Overbars in Equations (1), (2) and (4) refer to the Reynold averaging operator and the (') the fluctuation term.

3. Results and Discussion

3.1. Annual Cycle

Figure 2 presents the 2023 half-hourly annual cycle of weather and surface conditions obtained for the first time at this location. As it can be seen in **Figure 2(a)**, the first rainy event in 2023 occurred unexpectedly during the dry season, in January, bringing 16.9 mm of precipitation. This slightly reduced the incoming shortwave radiation (SWin), but not to the same magnitude as what was observed between July and August (**Figure 2(b)**). Rainfall events remained sporadic until March, when they became more frequent until June and July. Following a brief hiatus with limited number of events between July and August, there was a restart of rainy events from September until nearly the end of the year, indicating the short wet season (**Figure 2(a)**). The months of June and July were identified as the months with the highest precipitation, recording over 400 mm of rainfall (**Figure 3**), contributing to an annual total of 1440 mm.

Despite the amount of rainfall and yearly distribution of rainy events, the annual cycle of the 2023-year was also notably characterized by elevated air and underground temperatures values, even at a depth of 30 cm (**Figure 2(c)**, **Figure**

2(d)). The soil temperature at 30 cm depth consistently exceeded 25˚C indicating how warm this soil layer was (**Figure 2(d)**). At ~5 cm under the ground, the maximum recorded temperature reached approximatively 45.32˚C in May. Obviously the amount of rainfall (547 mm) fallen between January and May 2023 was not sufficient to lower the underground temperature at this depth (**Figure 2(d)**). The Volumetric soil Water Content (VWC) at the four distinct layers (5, 10, 20 and 30 cm) corresponded closely with precipitation dynamics, exhibiting values ranging from 0.017 and 0.208 $cm^3 \cdot cm^{-3}$ (5 cm); 0.04 and 0.275 $cm^3 \cdot cm^{-3}$ (10 cm); 0.04 and 0.2625 $cm^3 \cdot cm^{-3}$ (20 cm); 0.104 and 0.33 $cm^3 \cdot cm^{-3}$ (30 cm).

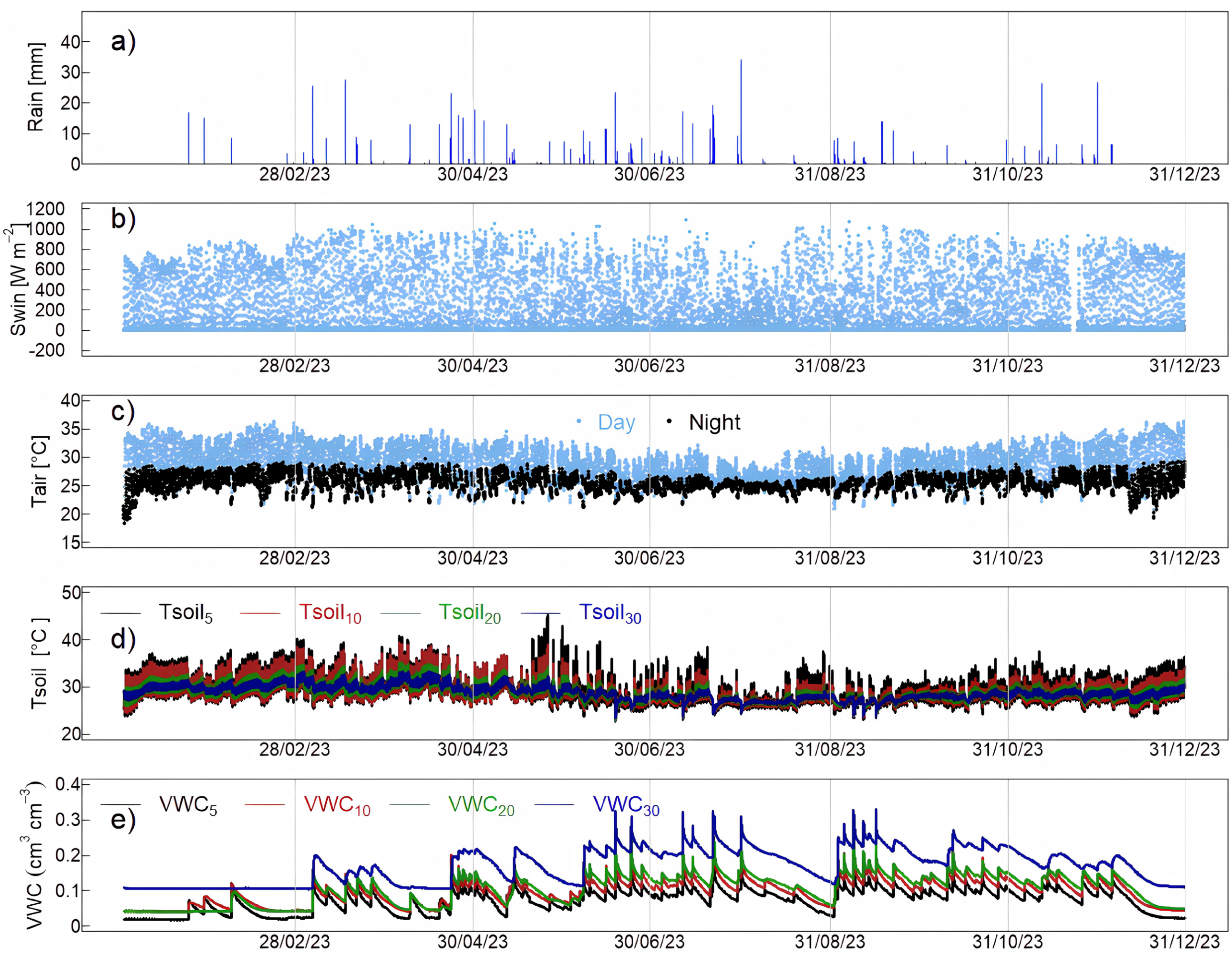

Figure 2. Temporal dynamics of the half-hourly measurements of: (a) rainfall; (b) incoming shortwave radiation; (c) air temperature during the daytime (blue color) and nighttime (black color); (d) soil temperature at 5 cm (black), 10 cm (red), 20 cm (green), and 30 cm (blue) depths, respectively; (e) volumetric soil water content at 5 cm (black), 10 cm (red), 20 cm (green), and 30 cm (blue) depths, respectively, during the 2023-year.

The diurnal daily range of air temperature never goes below 5˚C evidencing indeed the warmest state of the air during the 2023-year at the site (**Figure 2(c)**). This is similar to what was observed at another site near this one but during the 2021-year [33]. The air and underground temperature dynamics (**Figure 2(c)**, **Figure 2(d)**) follow nearly those of incoming shortwave and outgoing longwave radiations. They increase at the beginning of the year to reach their first maximum in March (~1040 and ~550 W·m^{-2} respectively) and their lowest annual magnitudes (~500 and ~450 W·m^{-2} respectively) were observed during the short dry season (between July and August) characterized by a rapid decrease (from ~0.3 to ~0.1 cm^3·cm^{-3}) of the volumetric water content at 30 cm depth (**Figure 2(e)**).

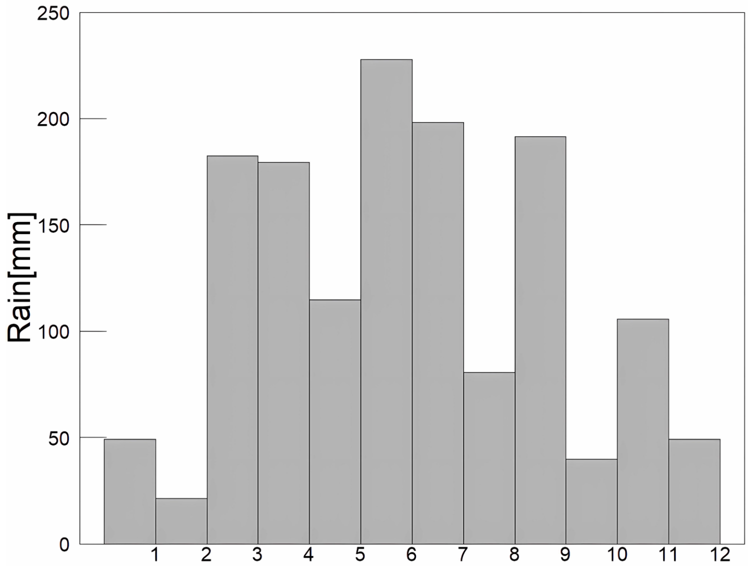

Figure 3. Monthly cumul of precipitation at the site during the studied year.

3.2. Energy Balance Components

Figure 4 illustrates the half-hourly energy balance components along the 2023-year. The half-hourly fluxes obtained with eddy covariance were not gap filled.

The results show that over the entire year, *Rnet* is below 800 W·m^{-2} with a pronounced seasonal behavior. We can observe higher values of *Rnet* mainly occurring in March (650 W·m^{-2}) and December (610 W·m^{-2}) with somehow more available energy to the partitioning into soil heat flux (*G*), sensible heat (*H*) and latent heat (*LE*) fluxes. The lowest values of *Rnet* (<500 W·m^{-2}) happen in June, July, August and September alike the incoming shortwave radiation (**Figure 2(b)**). These months coincide with periods with low level cloud [37] which diminishes radiation and consequently less available energy to be dissipated into convective fluxes (heat and water vapor exchanges). More details characterizing the radiation characteristics and patterns near the site can be found in [30].

Surprisingly, the soil heat flux (*G*) did not follow precipitation dynamics and stayed high even during months when water availability was elevated (**Figure 2(e)**). Its lowest value was observed however in August, a "relatively dry" month with less solar radiation at the surface [30] [37]. The sensible heat flux showed a pronounced seasonal cycle with a maximum of (~220 W·m^{-2}) between January and March during the warmest months and a daytime minimum of 60 W·m^{-2} occurring during the wet months. Aside periods with relatively long gaps, the amount of the latent heat flux (*LE*) was important (**Figure 4(c)**) during months with high soil and air temperatures and even during low soil water content (**Figure 2(c)**, **Figure 2(d)**). It also appears from the annual cycle that more available energy was converted into actual evapotranspiration (AET) as this is expected for this tropical humid site (RH > 50% all year long). During the studied year, the highest rate of water loss through actual evapotranspiration (~350 W·m^{-2}) was observed between March-May and November-December.

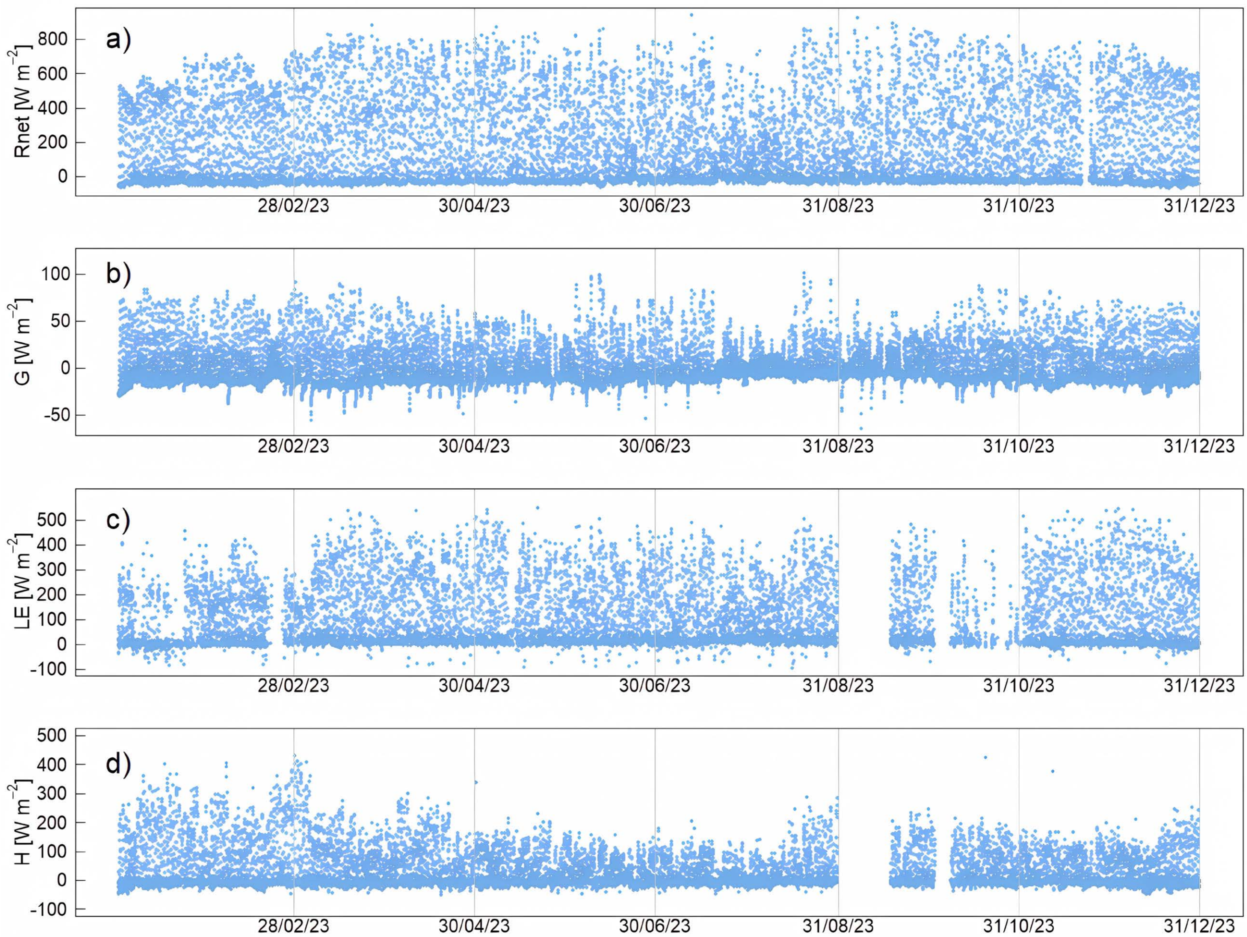

Figure 4. Temporal dynamics of the half-hourly measurements of: (a) net radiation; (b) soil heat; (c) latent heat and (d) sensible heat fluxes at the site.

Linear regression of turbulent fluxes ($H + LE$) against available energy ($Rnet - G$) (**Figure 5**) was used to evaluate the energy balance closure of the 2023-year. The slope was 0.77, which indicates that the turbulent fluxes were underestimated when compared to the available energy. The intercept was 15.74 W·m^{-2} and R^2, 0.90. These values are however close to those available in literature where authors often reported that ($LE + H$) were underestimated by 10% - 30% [38], which stem from unaccounted processes such as advection, neglected energy sink or even sampling error [23]. The energy balance closure presented in this study is similar to what is commonly found with eddy covariance method in previous studies [38] and especially in the West African humid regions [20] [26] [39].

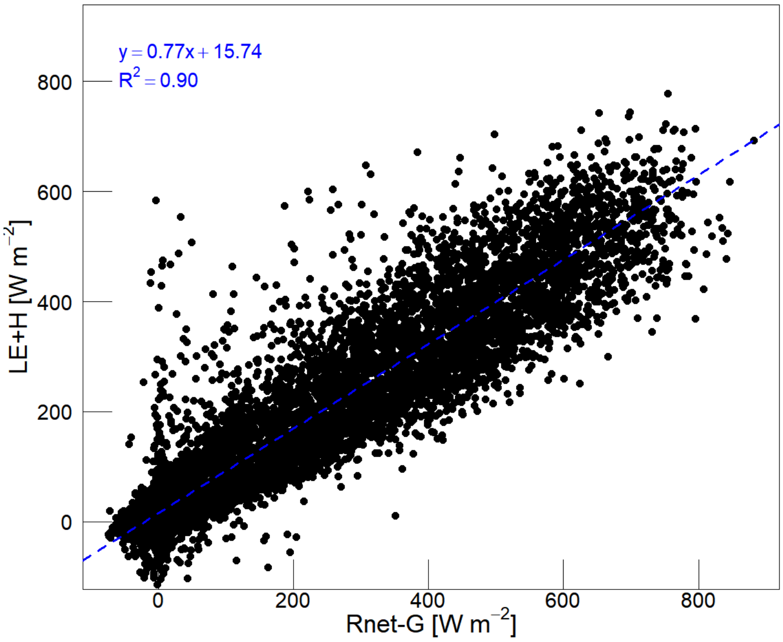

Figure 5. Energy balance closure for the 2023 year at the site.

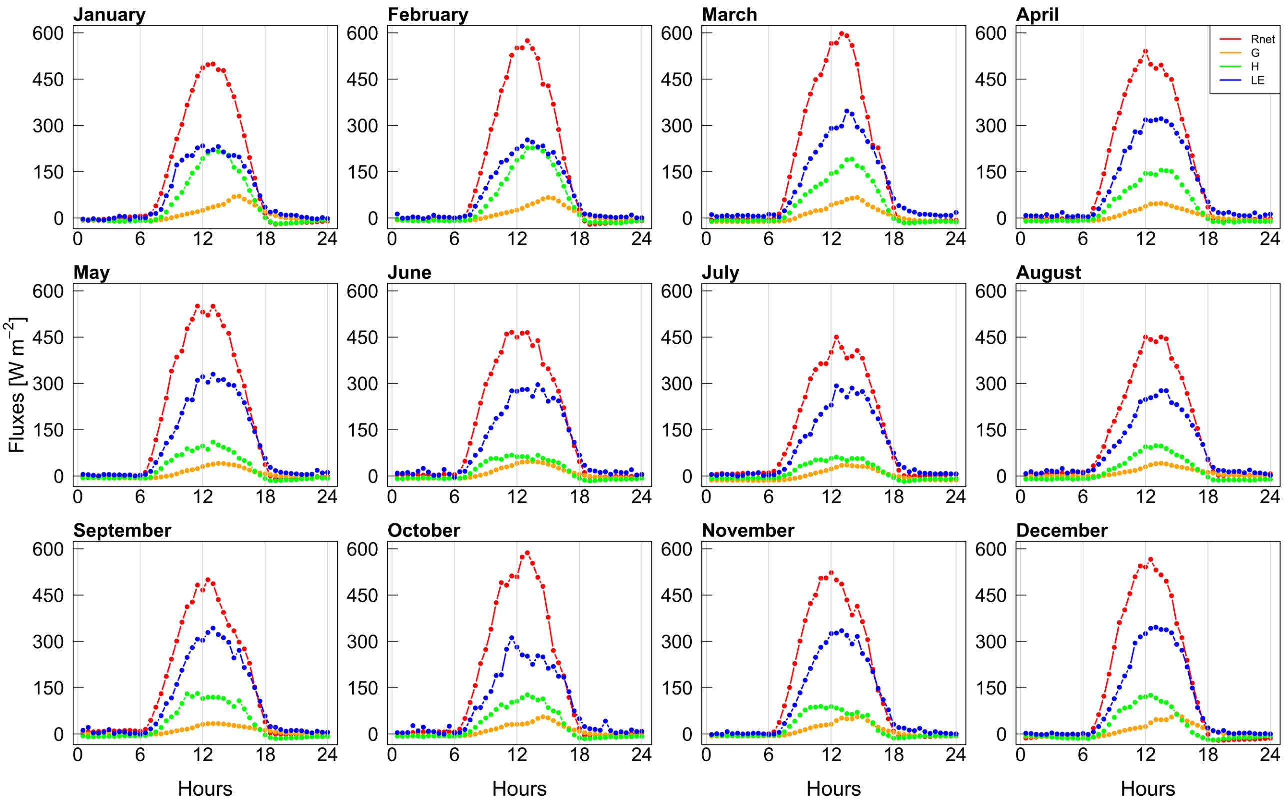

Figure 6. Monthly diurnal cycles of the energy balance components throughout the 2023 year at the site. Net radiation (*Rnet*, red), latent heat (*LE*, blue), sensible heat (*H*, green) and soil heat (*G*, orange) fluxes.

In **Figure 6**, the monthly mean diurnal cycles of net radiation, soil heat, sensible and latent heat fluxes, computed from the half-hourly data, deviate in accordance with the change of seasons. *Rnet* shows an almost symmetric pattern, more in December and January, typical of clear sky conditions [30]. However, it owned two highest daily maximums (650 and 610 W·m^{-2}) reached respectively in March and December, while the lowest daily minimum (440 W·m^{-2}) occurred in July-August. The soil heat flux (*G*) acquired with the sensor was not in phase with the daily course of net radiation and had relatively low values despite the high temperature gradient in the soil. **Figure 6** reveals also that the latent heat flux provides the most atmospheric moisture (350 W·m^{-2}) throughout the year, and stays higher than 200 W·m^{-2} across the year. The sensible heat flux was not negligible with an apparent seasonality that follows the precipitation regime.

3.3. Net Ecosystem Exchange

Figure 7 displays the half-hourly values of the net ecosystem exchange (*NEE*) during the 2023-year. Note that gaps in the yearly measurements of *NEE* were not filled in this study. *NEE* varied to a large extent during the observational period that ranged from ~−25 μmol·m^{-2}·s^{-1} to ~10 μmol·m^{-2}·s^{-1}. Carbon uptake by the ecosystem (negative values of *NEE*) followed closely the precipitation regime (**Figure 2(a)**; **Figure 3**). At the beginning of the year, it increases (in absolute value) gradually with rainy events to reach a maximum of about −22 μmol·m^{-2}·s^{-1} on average between April and May, then decreases slowly after with the diminution of rainfall (**Figure 3**), before starting to increase concomitantly to the rainfall to nearly the end of the year. However, the positive values remain almost constant, with an average of ~8 μmol·m^{-2}·s^{-1}. This suggests that at this time step that environmental and climate conditions seems to not affect mostly the nighttime CO_2 fluxes at the site. The nighttime *NEE* values obtained at the oil palm site were slightly higher compared to those (~6 μmol·m^{-2}·s^{-1}) found by [27] above a degraded woodland in sudanian climate (~1200 mm/y average of rainfall). However, they were close to values (~8.2 μmol·m^{-2}·s^{-1}) observed over a clear forest site [28] located also in sudanian climate. When rain become regular, CO_2 uptake increases and when soil moisture reaches a sufficient and almost stable level, from May to June, assimilation carries on and even continues to increase regularly, suggesting

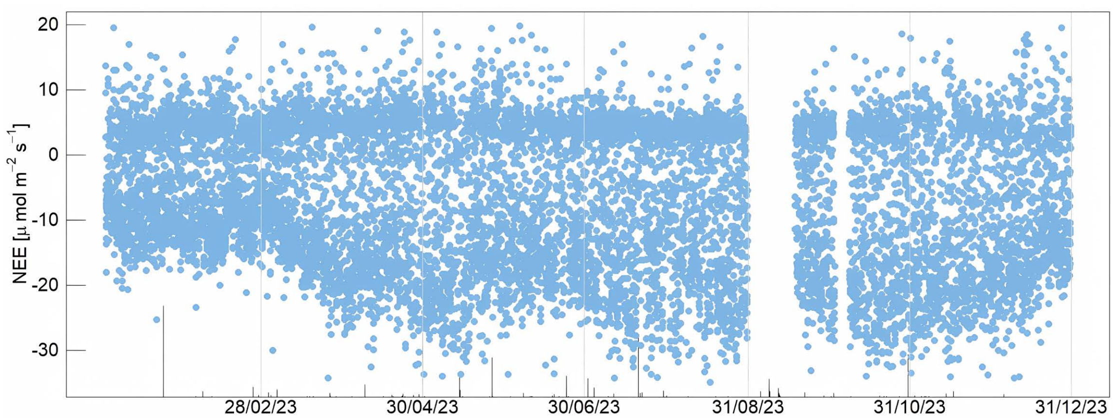

Figure 7. Temporal dynamic of the net ecosystem exchanges at the oil palm site Dangbo site during the 2023-year.

continuous growth of vegetation. Finally, the maximum values of the daytime averages of *NEE* was lower than those reported above the forest site (28.2 ± 1.2 μmol·m^{-2}·s^{-1}) [28] but higher than uptake from a cultivated savannah (17.6 ± 0.8 μmol·m^{-2}·s^{-1}) [25].

4. Conclusion

This study is the first continuous CO_2, H_2O and energy flux measurements above the oil palm plantation using the eddy covariance technique, to our knowledge, in Africa. The first outcomes of this study enable us to gain insight into the seasonal dynamics of these exchanges in southeastern Benin. Their dynamics seem indeed to be controlled by the rainfall regime. At the beginning of the 2023 year, the latent heat flux increases from 233 W·m^{-2} in January to reach its first annual maximum (350 W·m^{-2}) in March, concomitantly with the net radiation before experiencing a slight decrease induced by a decrease in the available energy at the surface. Results also showed that the turbulent carbon dioxide flux remains important with more absorption of CO_2 from the atmosphere into the vegetation during periods with regular rainy events. On average, nighttime CO_2 emissions were close to those observed over a forest site, while the daytime uptake was lower. However, the author cautions against this comparison due to differences in both the analyzed years and climate. Further investigations are needed to gain a valuable understanding of the physical processes which occur within this ecosystem.

Acknowledgements

The author thanks the OWSD Early Career Fellowship which funds this eddy covariance site.

Conflicts of Interest

The author declares no conflicts of interest regarding the publication of this paper.

References

[1] Chiriacò, M.V., Galli, N., Santini, M. and Rulli, M.C. (2024) Deforestation and Greenhouse Gas Emissions Could Arise When Replacing Palm Oil with Other Vegetable Oils. *Science of the Total Environment*, **914**, Article ID: 169486. https://doi.org/10.1016/j.scitotenv.2023.169486

[2] Cooper, H.V., Evers, S., Aplin, P., Crout, N., Dahalan, M.P.B. and Sjogersten, S. (2020) Greenhouse Gas Emissions Resulting from Conversion of Peat Swamp Forest to Oil Palm Plantation. *Nature Communications*, **11**, Article No. 407. https://doi.org/10.1038/s41467-020-14298-w

[3] Germer, J. and Sauerborn, J. (2007) Estimation of the Impact of Oil Palm Plantation Establishment on Greenhouse Gas Balance. *Environment, Development and Sustainability*, **10**, 697-716. https://doi.org/10.1007/s10668-006-9080-1

[4] Intergovernmental Panel on Climate Change (IPCC) (2023) Climate Change 2022—Impacts, Adaptation and Vulnerability: Working Group II Contribution to the Sixth Assessment Report of the Intergovernmental Panel on Climate Change. Cambridge

University Press. https://doi.org/10.1017/9781009325844

[5] Intergovernmental Panel on Climate Change (IPCC) (2023) Climate Change 2021—The Physical Science Basis: Working Group I Contribution to the Sixth Assessment Report of the Intergovernmental Panel on Climate Change. Cambridge University Press. https://doi.org/10.1017/9781009157896

[6] Kogan, F. (2022) The IPCC Reports on Global Warming and Land Changes. In: Kogan, F., Ed., *Remote Sensing Land Surface Changes*: *The* 1981-2020 *Intensive Global Warming*, Springer International Publishing, 67-79. https://doi.org/10.1007/978-3-030-96810-6_3

[7] Chen, J.M. (2021) Carbon Neutrality: Toward a Sustainable Future. *The Innovation*, **2**, Article ID: 100127. https://doi.org/10.1016/j.xinn.2021.100127

[8] Finkbeiner, M. and Bach, V. (2021) Life Cycle Assessment of Decarbonization Options—Towards Scientifically Robust Carbon Neutrality. *The International Journal of Life Cycle Assessment*, **26**, 635-639. https://doi.org/10.1007/s11367-021-01902-4

[9] Gil, L. and Bernardo, J. (2020) An Approach to Energy and Climate Issues Aiming at Carbon Neutrality. *Renewable Energy Focus*, **33**, 37-42. https://doi.org/10.1016/j.ref.2020.03.003

[10] Huang, M. and Zhai, P. (2021) Achieving Paris Agreement Temperature Goals Requires Carbon Neutrality by Middle Century with Far-Reaching Transitions in the Whole Society. *Advances in Climate Change Research*, **12**, 281-286. https://doi.org/10.1016/j.accre.2021.03.004

[11] Chen, L., Msigwa, G., Yang, M., Osman, A.I., Fawzy, S., Rooney, D.W., *et al*. (2022) Strategies to Achieve a Carbon Neutral Society: A Review. *Environmental Chemistry Letters*, **20**, 2277-2310. https://doi.org/10.1007/s10311-022-01435-8

[12] Chu, H., Baldocchi, D.D., John, R., Wolf, S. and Reichstein, M. (2017) Fluxes All of the Time? A Primer on the Temporal Representativeness of Fluxnet. *Journal of Geophysical Research*: *Biogeosciences*, **122**, 289-307. https://doi.org/10.1002/2016jg003576

[13] Rival, A. and Levang, P. (2014) Palms of Controversies: Oil Palm and Development Challenges. CIFOR.

[14] Koussihouèdé, H., Clermont-Dauphin, C., Aholoukpè, H., Barthès, B., Chapuis-Lardy, L., Jassogne, L., *et al*. (2019) Diversity and Socio-Economic Aspects of Oil Palm Agroforestry Systems on the Allada Plateau, Southern Benin. *Agroforestry Systems*, **94**, 41-56. https://doi.org/10.1007/s10457-019-00360-0

[15] Yan, W. (2017) A Makeover for the World's Most Hated Crop. *Nature*, **543**, 306-308. https://doi.org/10.1038/543306a

[16] Bonan, G.B., Lucier, O., Coen, D.R., Foster, A.C., Shuman, J.K., Laguë, M.M., *et al*. (2024) Reimagining Earth in the Earth System. *Journal of Advances in Modeling Earth Systems*, **16**, e2023MS004017. https://doi.org/10.1029/2023ms004017

[17] Zarakas, C.M., Kennedy, D., Dagon, K., Lawrence, D.M., Liu, A., Bonan, G., Koven, C.D., Lombardozzi, D. and Swann, A.L.S. (2024) Land Processes Can Substantially Impact the Mean Climate State. https://eartharxiv.org/repository/view/6605/

[18] Dislich, C., Keyel, A.C., Salecker, J., Kisel, Y., Meyer, K.M., Auliya, M., *et al*. (2016) A Review of the Ecosystem Functions in Oil Palm Plantations, Using Forests as a Reference System. *Biological Reviews*, **92**, 1539-1569. https://doi.org/10.1111/brv.12295

[19] Mamadou, O., Galle, S., Cohard, J., Peugeot, C., Kounouhewa, B., Biron, R., *et al*. (2016) Dynamics of Water Vapor and Energy Exchanges above Two Contrasting Sudanian Climate Ecosystems in Northern Benin (west Africa). *Journal of Geophysical*

Research: *Atmospheres*, **121**, 11,269-11,286. https://doi.org/10.1002/2016jd024749

[20] Mamadou, O., Cohard, J.M., Galle, S., Awanou, C.N., Diedhiou, A., Kounouhewa, B., *et al*. (2014) Energy Fluxes and Surface Characteristics over a Cultivated Area in Benin: Daily and Seasonal Dynamics. *Hydrology and Earth System Sciences*, **18**, 893-914. https://doi.org/10.5194/hess-18-893-2014

[21] Aubinet, M., Grelle, A., Ibrom, A., Rannik, Ü., Moncrieff, J., Foken, T., *et al*. (1999) Estimates of the Annual Net Carbon and Water Exchange of Forests: The EUROFLUX Methodology. *Advances in Ecological Research*, **30**, 113-175. https://doi.org/10.1016/s0065-2504(08)60018-5

[22] Aubinet, M., Vesala, T. and Papale, D. (2012) Eddy Covariance: A Practical Guide to Measurement and Data Analysis. Springer Science & Business Media.

[23] Baldocchi, D.D. (2019) How Eddy Covariance Flux Measurements Have Contributed to Our Understanding of *global Change Biology*. *Global Change Biology*, **26**, 242-260. https://doi.org/10.1111/gcb.14807

[24] Ajao, A.I., Jegede, O.O. and Ayoola, M.A. (2019) Diurnal and Seasonal Variability of Sensible and Latent Heat Fluxes at an Agricultural Site in Ile-Ife, Southwest Nigeria. *Theoretical and Applied Climatology*, **139**, 1237-1246. https://doi.org/10.1007/s00704-019-03043-z

[25] Ago, E.E., Agbossou, E.K., Galle, S., Cohard, J., Heinesch, B. and Aubinet, M. (2014) Long Term Observations of Carbon Dioxide Exchange over Cultivated Savanna under a Sudanian Climate in Benin (West Africa). *Agricultural and Forest Meteorology*, **197**, 13-25. https://doi.org/10.1016/j.agrformet.2014.06.005

[26] Quansah, E., Mauder, M., Balogun, A.A., Amekudzi, L.K., Hingerl, L., Bliefernicht, J., *et al*. (2015) Carbon Dioxide Fluxes from Contrasting Ecosystems in the Sudanian Savanna in West Africa. *Carbon Balance and Management*, **10**, Article No. 1. https://doi.org/10.1186/s13021-014-0011-4

[27] Ago, E.E., Serça, D., Agbossou, E.K., Galle, S. and Aubinet, M. (2015) Carbon Dioxide Fluxes from a Degraded Woodland in West Africa and Their Responses to Main Environmental Factors. *Carbon Balance and Management*, **10**, Article No. 22. https://doi.org/10.1186/s13021-015-0033-6

[28] Ago, E.E., Agbossou, E.K., Cohard, J., Galle, S. and Aubinet, M. (2016) Response of CO_2 Fluxes and Productivity to Water Availability in Two Contrasting Ecosystems in Northern Benin (West Africa). *Annals of Forest Science*, **73**, 483-500. https://doi.org/10.1007/s13595-016-0542-9

[29] Beck, H.E., Zimmermann, N.E., McVicar, T.R., Vergopolan, N., Berg, A. and Wood, E.F. (2018) Present and Future Köppen-Geiger Climate Classification Maps at 1-Km Resolution. *Scientific Data*, **5**, Article No. 180214. https://doi.org/10.1038/sdata.2018.214

[30] Mamadou, O., Mariscal, A., Koukoui, D.R.R., Hounsinou, M. and Kounouhéwa, B. (2024) Meteorological Conditions and Second-Order Moments of Wind Speed Components over a Nonuniform Terrain in Dangbo, Southeastern Benin. *Meteorology and Atmospheric Physics*, **136**, Article No. 47. https://doi.org/10.1007/s00703-024-01043-x

[31] Dadi, R., Mamadou, O. and Ago, E.E. (2022) Inventaire floristique et occupation du sol sur le site de mesure des flux de Dangbo (Sud-Est du Bénin). Rapport Technique, 37.

[32] Faure, P. and Volkoff, B. (1998) Some Factors Affecting Regional Differentiation of the Soils in the Republic of Benin (West Africa). *CATENA*, **32**, 281-306.

https://doi.org/10.1016/s0341-8162(98)00038-1

[33] Schotanus, P., Nieuwstadt, F.T.M. and De Bruin, H.A.R. (1983) Temperature Measurement with a Sonic Anemometer and Its Application to Heat and Moisture Fluxes. *Boundary-Layer Meteorology*, **26**, 81-93. https://doi.org/10.1007/bf00164332

[34] Moncrieff, J.B., Massheder, J.M., de Bruin, H., Elbers, J., Friborg, T., Heusinkveld, B., *et al*. (1997) A System to Measure Surface Fluxes of Momentum, Sensible Heat, Water Vapour and Carbon Dioxide. *Journal of Hydrology*, **188**, 589-611. https://doi.org/10.1016/s0022-1694(96)03194-0

[35] Mauder, M. and Foken, T. (2004) Documentation and Instruction Manual of the Eddy Covariance Software Package TK2. https://epub.uni-bayreuth.de/id/eprint/884/1/ARBERG026.pdf

[36] Stull, R.B. (1988) An Introduction to Boundary Layer Meteorology. Kluwer Academic Publishers. https://doi.org/10.1007/978-94-009-3027-8

[37] Matthew, O.J., Ayoola, M.A., Ogolo, E.O. and Sunmonu, L.A. (2020) Impacts of Cloudiness on Near Surface Radiation and Temperature in Nigeria, West Africa. *SN Applied Sciences*, **2**, Article No. 2127. https://doi.org/10.1007/s42452-020-03961-y

[38] Wilson, K., Goldstein, A., Falge, E., Aubinet, M., Baldocchi, D., Berbigier, P., *et al*. (2002) Energy Balance Closure at FLUXNET Sites. *Agricultural and Forest Meteorology*, **113**, 223-243. https://doi.org/10.1016/s0168-1923(02)00109-0

[39] Mamadou, O. (2014) Etude des flux d'Evapotranspiration en climat soudanien: comportement comparé de deux couverts végétaux au Bénin. Ph.D. Thesis, Université de Grenoble (France) et Université d'Abomey-Calavi (Bénin).